CFD Analysis of Three Dimensional Natural Convection and Entropy Generation in Triangular Cavity with Inserted Isothermal Heater

Walid Aich

Mechanical Engineering Department, University of Ha'il, Kingdom of Saudi Arabia
Research Unit of Materials, Energy and Renewable Energies (MEER), Tunisia
E-mail address: *aich_walid@yahoo.fr*

ABSTRACT

A three-dimensional numerical analysis of laminar natural convection with entropy generation in an air filled triangular enclosure with inserted isothermal heater at the bottom wall has been carried out using finite volume method. The aim of the study is to investigate how buoyancy forces influence air flow and temperature patterns inside the cavity cooled on its inclined wall while all other walls are assumed to be perfect thermal insulators. Rayleigh number is the main parameter which varies from 10^3 to 10^5 and Prandtl number is fixed at Pr =0.71. Results are reported in terms of particles trajectories, iso-surfaces of temperature, mean Nusselt number entropy generated and Bejan number. It has been found that the value of Rayleigh number is effective on temperature distribution, flow field and heat transfer.

Keywords: 3D; CFD; Natural convection; entropy generation; inserted heater; Rayleigh number; Nusselt number.

1. INTRODUCTION

Analysis of natural convection flow and heat transfer in enclosures plays important role in many diverse applications including solar collectors, building heating and ventilation, cooling electronical devices, cryogenic storage, nuclear reactor design and furnace design. Cooling of electronic equipment must be considered when designing such systems. In the open literature, many studies have appeared on natural convection in triangular enclosures due to its wide applications. The pioneers of natural convection studying in triangular cavities are Flack (1983) and Poulikakos and Bejan (1983a, 1983b). Then, Asan and Namli (2000, 2001) modeled the winter and summer day boundary conditions inside a roof of triangular cross-section. Joudi *et al* . (2004) studied the performance of a prism shaped storage solar collector with a right triangular cross sectional area for the hot inclined wall and well insulated bottom and vertical walls. It was found that, early in the day, the temperature distribution is symmetric due to the low velocity, which is insufficient to circulate the fluid within the system. However, as the day progressed, the convective effects become more prominent leading to the distortion of isotherms. Further, it was found that the insertion of a horizontal partition within the storage collector enhances stratification of the water and renders higher mean tank temperature and higher stored energy. Ridouane *et al.* (2005) investigated the laminar natural convection in the air filled right-angled triangular enclosure with the hot vertical wall, cold inclined wall and adiabatic horizontal wall. It was found that, the heat transfer rate within the enclosure enhances largely with the decrease in both the apex angle and Rayleigh number.

Oztop *et al.* (2007) examined the convective heat transfer and fluid flow in a shed roof with or without eave for the summer boundary conditions. It was observed that the heat transfer rate from the inclined wall to the

bottom wall increases as the eave length increases. Also, it was found that the presence of the eave in the shed roof increases the heat transfer rate. Varol *et al.* (2006) carried out the natural convection problem with flush mounted heater on one wall of a triangular cavity. Governing parameters on heat transfer and flow fields are aspect ratio of triangle, location of heater, length of heater and Rayleigh number. They observed that the most important parameter on heat transfer and flow field is the position of heater which can be a control parameter for their system. Salmun (1995) reported convection patterns in a triangular enclosure filled with air (Pr= 0.72) or water (Pr= 7.1) for various aspect ratios in the presence of the hot bottom wall, cold hypotenuse and adiabatic vertical wall. It was observed that, at the low Ra, the changes in the aspect ratio had the negligible effect on the stream function and isotherms within the enclosure. However, the changes in the aspect ratio do affect the flow pattern and temperature fields significantly at the high Ra.

The fluid motion is found to be more intense in the right half of the enclosure and hence, the size of streamline circulation cells is observed to increase in size near those regions. Sojoudi *et al.* (2016) carried out the numerical simulations in order to study the unsteady air flow and heat transfer in a partitioned triangular cavity which was differentially heated from the left inclined wall. Also, an additional heat source was placed at the bottom wall of the triangular cavity. It was found that the thermal boundary layer thickness is increased along the left wall for the greater heater size and that the variation of Ra does not have any significant effect on the heat transfer rate of the left wall which decreases with time. A sizable amount of other related studies can be found in the literature review (Basak *et al.*, 2007; Roy *et al.*, 2008; Kent, 2009).

Moreover, only limited attention has been paid to the study of three-dimensional transverse flow which is primordial when dealing with the enhancement of heat transfer. The paramount aim of this work has been to numerically investigate the diffusive natural convection heat transfer and fluid flow in a three-dimensional air filled triangular enclosure with inserted isothermal heater.

2. MATHEMATICAL FORMULATION

2.1 Physical model

Physical model is presented in Fig. 1 with its specified coordinate system and boundary conditions. Indeed, the considered problem is three-dimensional natural convection and entropy generation in an air filled triangular cavity with inserted isothermal heater at the bottom wall. The analyzed cavity is cooled on its inclined wall while remaining walls are assumed to be insulated.

2.2 Governing Equations and Numerical Solution

As numerical method we had recourse to the vorticity-potential vector formalism $(\vec{\psi} - \vec{\omega})$ which allows, in a three-dimensional configuration, the elimination of the pressure, which is a delicate term to treat. To eliminate this term one applies the rotational to the equation of momentum. More details on this 3-D formalism can be found in the work of Kolsi *et al.* (2007).
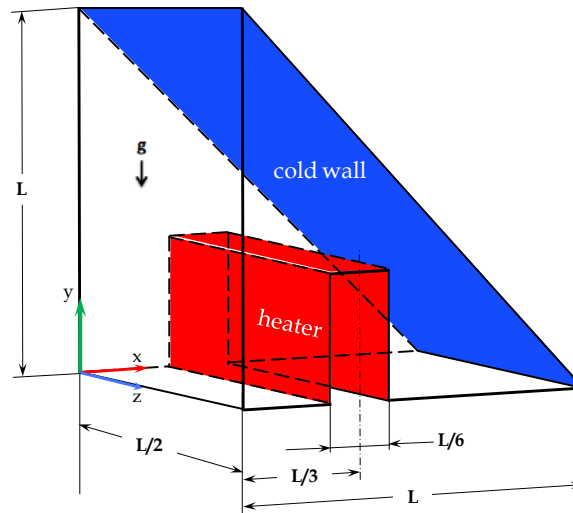
Fig. 1: Schematic of an air filled triangular enclosure

The potential vector and the vorticity are respectively defined by the two following relations:

$$\vec{\omega}' = \vec{\nabla} \times \vec{V}' \quad \text{and} \quad \vec{V}' = \vec{\nabla} \times \vec{\psi}' \tag{1}$$

After adimensionalisation the system of equations controlling the phenomenon becomes:

$$-\vec{\omega} = \nabla^2 \vec{\psi} \tag{2}$$

$$\frac{\partial \vec{\omega}}{\partial t} + (\vec{V}.\nabla)\vec{\omega} - (\vec{\omega}.\nabla)\vec{V} = \Delta\vec{\omega} + Ra.\Pr.\left[\frac{\partial T}{\partial z}; 0; -\frac{\partial T}{\partial x}\right] \tag{3}$$

$$\frac{\partial T}{\partial t} + \vec{V}.\nabla T = \Delta T \tag{4}$$

With: $\Pr = \dfrac{\nu}{\alpha}$ and $Ra = \dfrac{g.\beta.\Delta T.L^3}{\nu.\alpha}$

Boundary conditions for considered model are given as follows:

Temperature:

$T = 1$ on the inserted heater and $T = 0$ on the right inclined wall.

$\dfrac{\partial T}{\partial n} = 0$ on all other walls (adiabatic).

Velocity:

$V_x = V_y = V_z = 0$ on all walls

The generated entropy is written in the following form as: $S'_{gen} = -\dfrac{1}{T'^2}.\vec{q}.\vec{\nabla}T' + \dfrac{\mu}{T'}.\phi'$

The first term represents the generated entropy due to temperature gradient and the second that due to the friction effects.

$$\vec{q} = -k.\vec{grad}T$$

The dissipation function is written in incompressible flow as:

$$\phi' = 2\left[\left(\frac{\partial V'_x}{\partial x'}\right)^2 + \left(\frac{\partial V'_y}{\partial y'}\right)^2 + \left(\frac{\partial V'_z}{\partial z'}\right)^2\right] + \left(\frac{\partial V'_y}{\partial x'} + \frac{\partial V'_x}{\partial y'}\right)^2 + \left(\frac{\partial V'_z}{\partial y'} + \frac{\partial V'_y}{\partial z'}\right)^2 + \left(\frac{\partial V'_x}{\partial z'} + \frac{\partial V'_z}{\partial x'}\right)^2 \tag{5}$$

From where the generated entropy is written:

$$S'_{gen} = \frac{k}{T'^2_0}\left[\left(\frac{\partial T'}{\partial x'}\right)^2 + \left(\frac{\partial T'}{\partial y'}\right)^2 + \left(\frac{\partial T'}{\partial z'}\right)^2\right] + 2\frac{\mu}{T_0}\left\{\begin{array}{l}\left[\left(\frac{\partial V'_x}{\partial x'}\right)^2 + \left(\frac{\partial V'_y}{\partial y'}\right)^2 + \left(\frac{\partial V'_z}{\partial z'}\right)^2\right] \\ + \left(\frac{\partial V'_y}{\partial x'} + \frac{\partial V'_x}{\partial y'}\right)^2 + \left(\frac{\partial V'_z}{\partial y'} + \frac{\partial V'_y}{\partial z'}\right)^2 + \left(\frac{\partial V'_x}{\partial z'} + \frac{\partial V'_z}{\partial x'}\right)^2\end{array}\right\} \tag{6}$$

After adimensionalisation one obtains generated entropy number (dimensionless local entropy generated) which is written in the following way:

$$N_s = S'_{gen}\frac{1}{k}\left(\frac{LT_0}{\Delta T}\right)^2 \tag{7}$$

From where:

$$N_s = \left[\left(\frac{\partial T}{\partial x}\right)^2 + \left(\frac{\partial T}{\partial y}\right)^2 + \left(\frac{\partial T}{\partial z}\right)^2\right] + \varphi.\left\{2\left[\left(\frac{\partial V_x}{\partial x}\right)^2 + \left(\frac{\partial V_y}{\partial y}\right)^2 + \left(\frac{\partial V_z}{\partial z}\right)^2\right] + \left[\begin{array}{l}\left(\frac{\partial V_y}{\partial x} + \frac{\partial V_x}{\partial y}\right)^2 \\ + \left(\frac{\partial V_z}{\partial y} + \frac{\partial V_y}{\partial z}\right)^2 + \left(\frac{\partial V_x}{\partial z} + \frac{\partial V_z}{\partial x}\right)^2\end{array}\right]\right\} \tag{8}$$

With $\varphi = \dfrac{\mu\alpha^2 T_m}{L^2 k\Delta T^2}$ is the irreversibility coefficient.

The first term of N_s represents the local irreversibility due to the temperatures gradients, it is noted $N_{s\text{-th}}$. The second term represents the contribution of the viscous effects in the irreversibility it is noted $N_{s\text{-fr}}$. Ns give a good idea on the profile and the distribution of the generated local dimensionless entropy. The total dimensionless generated entropy is written:

$$S_{tot} = \int_v N_s \, dv = \int_v \left(N_{s-th} + N_{s-fr}\right)dv = S_{th} + S_{fr} \tag{9}$$

Bejan number (Be) is the ratio of heat and mass transfer irreversibility to the total generated entropy as:

$$Be = \frac{S_{th} + S_{dif}}{S_{th} + S_{fr} + S_{dif}} \tag{10}$$

Dimensionless irreversibilities distribution ratios (φ_1, φ_2 and φ_3), are given by:

$$\varphi_1 = \frac{\mu\alpha^2 T_0}{L^2 k \Delta T^2} \; ; \; \varphi_2 = \frac{RDT_0}{kC_0}\left[\frac{\Delta C'}{\Delta T'}\right]; \; \varphi_3 = \frac{RD}{k}\left[\frac{\Delta C'}{\Delta T'}\right] \tag{11}$$

The local and average Nusselt at the cold inclined wall are given by:

$$Nu = \frac{\partial T}{\partial n} \quad \text{and} \quad Nu_m = \int_0^{\sqrt{2}L}\int_0^L Nu\, dn\, dz \tag{12}$$

With: $\vec{n}$ is the unit vector normal to the cold inclined wall.

It should be noted that numerical analysis has been developed using an in-house computational code on the basis of FORTRAN programming language. The control volume finite difference method is used to discretize governing equations [(2)-(4)] and (8) respectively. The central-difference scheme is used for treating convective terms while the fully implicit procedure is used to discretize the temporal derivatives. The grids are considered uniform in all directions with clustering nodes on boundaries. The successive relaxation iteration scheme is used to solve the resulting non-linear algebraic equations.

A computer program written for a regular grid was improved to handle the irregularly shaped computational domain using the blocked-off method as described By Patankar (1981). In this technique, the whole region is divided into two active and inactive (blocked-off regions) parts. By this technique, the surface of inclined step in the present analysis is approximated by a series of fine cubic steps. It is obvious that using fine grids in the interface region between active and inactive zones causes to have an approximated boundary which is more similar to the true boundary. According to the blocked-off technique, known values of the dependent variables must be established in all inactive control volumes. If the inactive region represents a stationary solid boundary as in the case, the velocity components in that region must be equal to zero, and a known temperature (isothermal boundaries) must be established in the inactive control volumes. The control volumes, which are inside the active region, are designated as (1) and otherwise they are (0). The time step (10^{-4}) and spatial mesh ($81 \times 81 \times 41$) are utilized to carry out all the numerical tests. The solution is considered acceptable when the following convergence criterion is satisfied for each step of time:

$$\sum_i^{1,2,3} \frac{\max\left|\psi_i^n - \psi_i^{n-1}\right|}{\max\left|\psi_i^n\right|} + \max\left|T_i^n - T_i^{n-1}\right| \leq 10^{-4} \tag{13}$$

3. VALIDATION

The present model, in the form of an in-house computational fluid dynamics (CFD) code, has been validated successfully against the work of Yesiloz and Aydin (2013). Fig. 2 shows a good agreement in streamlines and isotherms of present study with published results.

4. RESULTS AND DISCUSSIONS

The iso-surfaces of temperature for different Rayleigh number values are shown in Fig. 3. For low values of Rayleigh number, the flow is weak due to quasi-conduction dominant heat transfer regime and air is nearly at rest. The isotherms present an almost vertical stratification near the left adiabatic wall and an inclined stratification near the cooled right side. It is obvious that these iso-surfaces are always orthogonal the adiabatic walls. By increasing Rayleigh number, heated air near the inserted heater is increasingly driven due to buoyancy forces making a plumelike temperature distribution formed from the heated block to the inclined wall due to convection regime of heat transfer. As it can be seen from the figure, Rayleigh number is an effective parameter on flow strength and a strong plumelike flow is observed near the left adiabatic wall with the increasing of this parameter.

Trajectories of particles for different Rayleigh number values are illustrated in Fig. 4. It is noted that Prandtl number is fixed at Pr = 0.71 for whole work and Rayleigh number is changed from 10^3 to 10^5. It can be seen from the figure that, for low values of Ra, three vortices are formed because heated air moves up from the heater and impinges to the cold inclined wall. For Ra = 10^3, a vortex is formed between left side of the heater and insulated vertical wall of triangular enclosure which rotates in counterclockwise direction.

Yesiloz and Aydin (2D) (2013)

Present Work (z=0.5 plan)
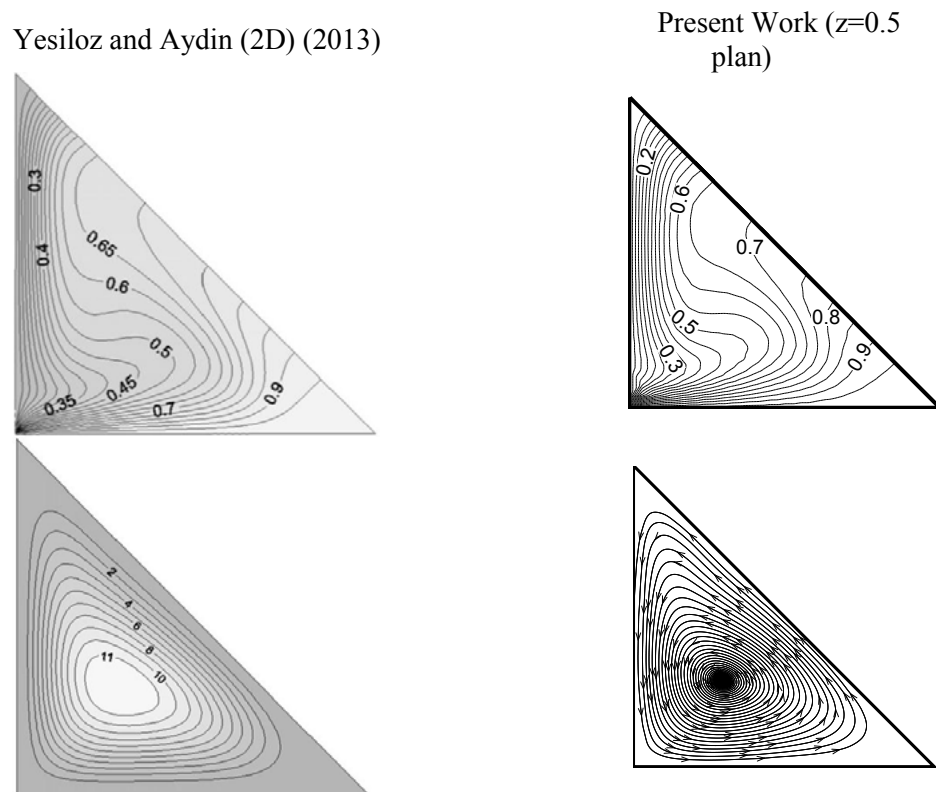
Fig. 2: Comparison with results of Yesiloz and Aydin (2013)

for Ra = 10^5 and Pr = 0.71
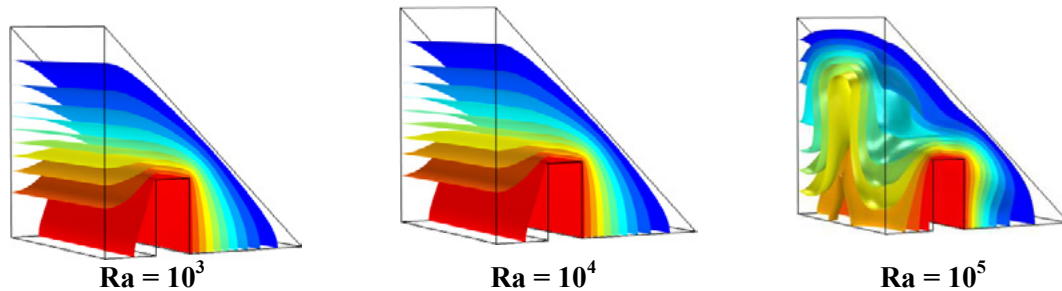
Fig. 3: Iso-surfaces of temperature for different Rayleigh number values
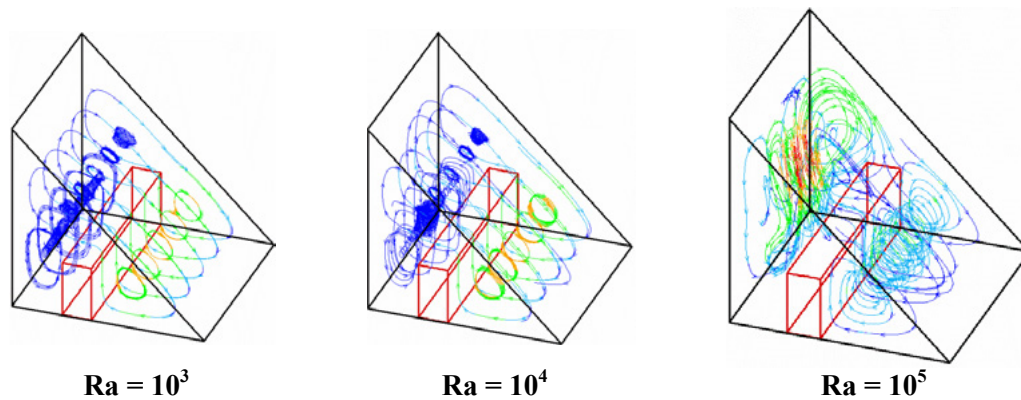
Fig. 4: Particles trajectory for different Rayleigh number values

Other two cells are obtained on the top of heater and right corner of the triangle enclosure. These are very similar for Ra =10^3 and Ra =10^4 due to quasi-conductive regime. Both top and right vortices rotate in clockwise direction due to rising fluid from heater to inclined wall. It rises and replaces with cooled fluid. The eye of vortices becomes almost in the same place with the increasing of Rayleigh number.

Trajectories of particles are more packed at the right side of the heater. It means that the flow moves faster as natural convection is intensified. As Rayleigh number increases (Ra = 10^5), velocity of fluid at the top of heater also increases due to increasing of effects of convection heat transfer regime. Increasing of Rayleigh number causes a denser clustering of temperature iso-surfaces and the three-dimensional character of the flow is more pronounced.

It is noticed that the rate of heat transfer inside the enclosure is measured in term of the overall Nusselt number. Therefore, fig. 5 shows the variation of the average Nusselt number, which characterizes the heat transfer from the inserted heater towards the vicinity of the enclosure, with the Rayleigh number. It is obvious that for low values of Ra and when the conduction is the dominant mode of heat transfer, this variation is insignificant. However, for $Ra \geq 10^4$ heat removal from the inserted heater increases by means of increasing Rayleigh number and the maximum rate is obtained for the highest Ra as expected. Indeed, by increasing Rayleigh number to 10^5, the fluid flow intensifies and the thermal energy transport increases due to the enhancement of convection heat transfer.

To achieve a maximum heat transfer rate between the inserted heater and the cooling air, it is essential to carry out an entropy generation analysis to investigate the two sources of irreversibilities that are responsible for heat losses. These irreversibilities are mainly due to heat transfer and fluid friction. Therefore, entropy generation due to heat transfer, the entropy generation due to friction and the total entropy generation as function of Rayleigh number are shown in fig. 6 for an irreversibility coefficient $\varphi = 10^{-5}$.
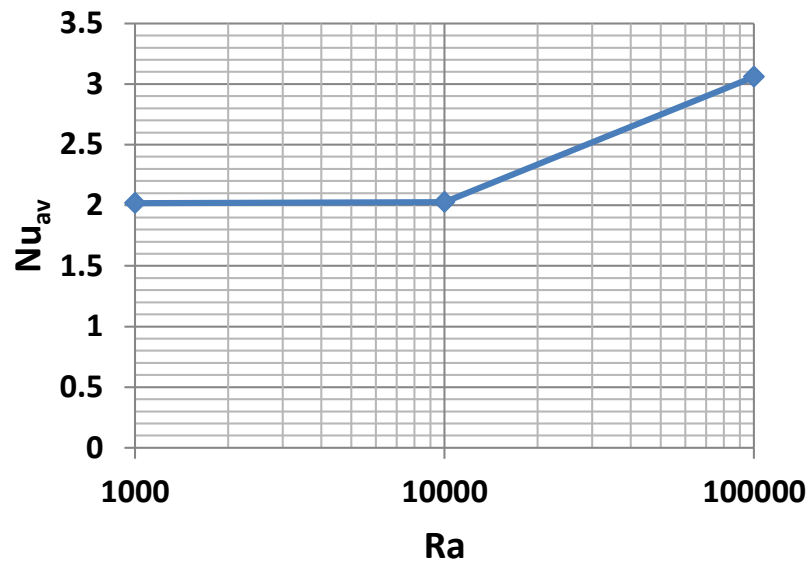
Fig. 5: Variation of Mean Nusselt number on cold wall with Rayleigh number
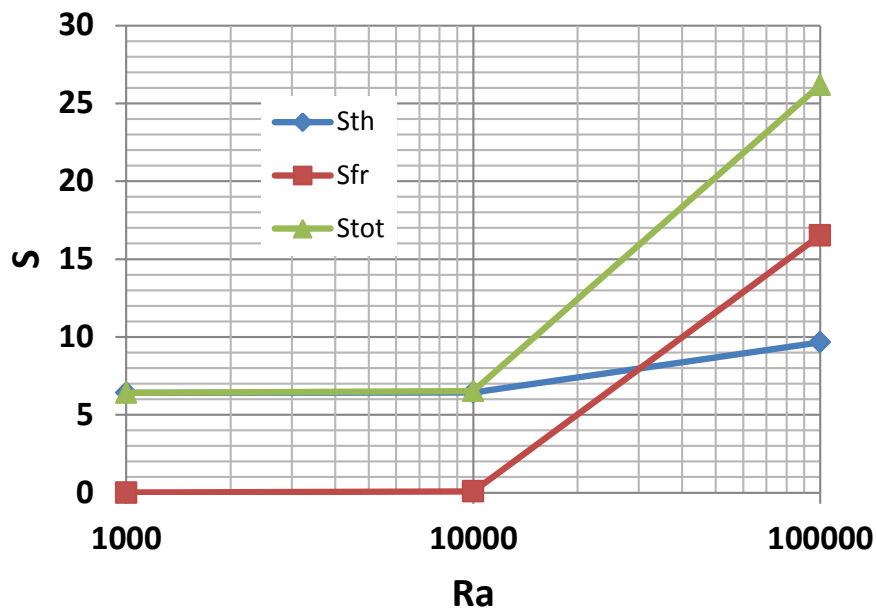
Fig. 6: Variations of entropy generations with Rayleigh number

For $Ra \leq 10^4$, entropy generation due to viscous irreversibility is less significant in deciding the total entropy generation, which is sum of entropy generations due to heat transfer and friction. Moreover, it can be observed that the entropy generation due to heat transfer and total entropy generation are equal which gives a clue that entropy due to heat transfer outweighs that due to fluid friction. However, an increasing of Ra ($Ra \geq 3*10^4$), fluid friction becomes the dominant cause of irreversibility and entropy generation due to viscous effects outweighs that due to heat transfer.

In order to better compare the magnitude of the two sources of irreversibilities, Fig. 7 illustrates the variation of Bejan number, which is the ratio of the heat transfer irreversibility to the total irreversibility. Indeed, the value of Be ranges from 0 to 1. Accordingly, Be = 0 and Be = 1 are two limiting cases indicating that the irreversibility is dominated by fluid friction and heat transfer, respectively. As shown from the figure, the highest value of Bejan number (almost 1) is obtained for the lowest Rayleigh number value (Ra = 10^3). It means that entropy generation due to fluid friction becomes insignificant and it is clear that irreversibility from heat transfer has dominant influence on resultant total entropy generation.
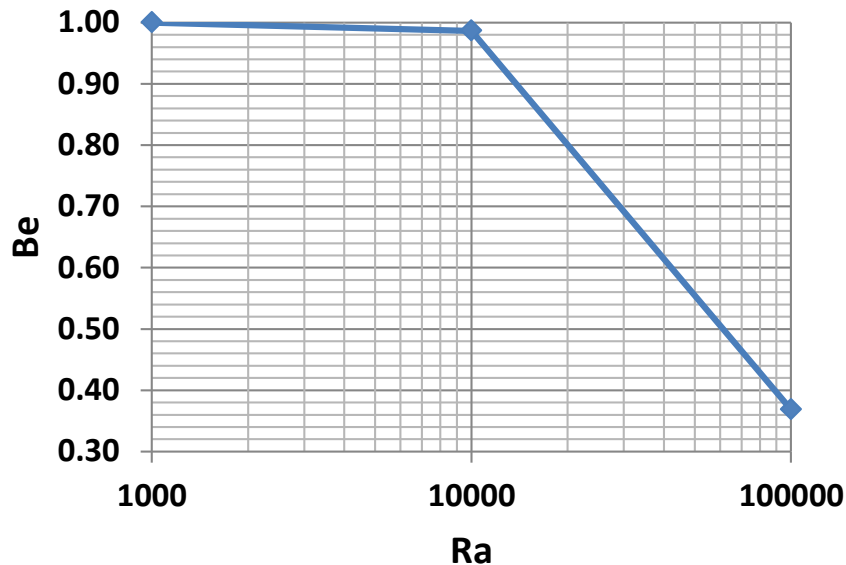
Fig. 7: Bejan number as function of Rayleigh number

5. CONCLUSIONS

Three-dimensional numerical investigation has been carried out to simulate natural convection and entropy generation in an air filled triangular cavity with inserted isothermal heater at the bottom wall. The analyzed cavity is cooled on its inclined wall while remaining walls are assumed to be insulated. Results are presented for different Rayleigh number values which is the main parameter of the study. In view of the obtained results, following findings may be summarized:

- For lower values of Rayleigh number, conduction is the primary mode of heat transfer and the flow strength is very low due to poor convective heat transfer.
- Flow strength increases with increasing of Rayleigh number and a strong convective current is noticeable along the inserted heater where cold air is heated.

- The flow structure and temperature distribution are sensitive to the value of Rayleigh number.
- Heat transfer is very weak at the left and top side of the heater when it is compared with the right side of the heater.
- Irreversibilities are mainly due to heat transfer at low Rayleigh number values and entropy generation due to fluid friction becomes more significant at high values.

Further study may include the effect parameters such as, heater height, heater width, heater location center and aspect ratio of triangular enclosure on heat transfer and fluid flow.

ACKNOWLEDGMENT

REFERENCES

ASAN, H. & NAMLI, L. (2000) Laminar natural convection in a pitched roof of triangular cross-section: summer day boundary conditions. Energy and Buildings, 33 (1), 69-73.

ASAN, H. & NAMLI, L. (2001) Numerical simulation of buoyant flow in a roof of triangular cross-section under winter day boundary conditions. Energy and Buildings, l33 (7), 753-757.

BASAK, T., ROY, S. & THIRUMALESHA, C. (2007) Finite element analysis of natural convection in a triangular enclosure: effects of various thermal boundary conditions. Chemical Engineering Science, 62 (9),2623-2640.

FLACK, R. D. (1980) The experimental measurement of natural convection heat transfer in triangular enclosures heated or cooled from bellow. Journal of Heat Transfer, 102 (4),770-772.

JOUDI, K.A., HUSSEIN, I.A. & FARHAN A.A. (2004) Computational model for a prism shaped storage solar collector with a right triangular cross section, Energy Convers. Manage, 45, 391-409.

KENT, E.F. (2009) Numerical analysis of laminar natural convection in isosceles triangular enclosures for cold base and hot inclined walls. Mechanics Research Communications, 36 (4), 497-508.

KOLSI, L., ABIDI, A., BORJINI, M.N., DAOUS, N. & BEN AISSIA, H. (2007) Effect of an external magnetic field on the 3-D unsteady natural convection in a cubical enclosure. Numerical Heat Transfer Part A, 51(10),1003-1021.

OZTOP, H.F., VAROL, Y. & KOCA, A. (2007) Laminar natural convection heat transfer in a shed roof with or without eave for summer season. Appl. Therm. Eng., 27, 2252-2265.

PATANKAR S.V. (1981) Numerical Heat Transfer and Fluid Flow. Philadelphia, USA, PA: Taylor & Francis.

POULIKAKOS, D. & BEJAN, A. (1983a) Natural convection experiments in a triangular enclosure. Journal of Heat Transfer, 105, 652-655.

POULIKAKOS, D. & BEJAN, A. (1983b) The fluid dynamics of an attic space. Journal of Fluid Mechanics, 131, 251-269.

RIDOUANE, E.H., CAMPO, A. & CHANG, J.Y. (2005) Natural convection patterns in right angled triangular cavities with heated vertical sides and cooled hypotenuses. J. Heat Transfer 127, 1181-1186.

ROY, S., BASAK, T., THIRUMALESHA, C. & KRISHNA, C.M. (2008) Finite element simulation on natural convection flow in a triangular enclosure due to uniform and non-uniform bottom heating. Journal of Heat Transfer, 130 (3), 1-10.

SALMUN, H. (1995) Convection patterns in a triangular domain. International Journal of Heat and Mass Transfer, 38 (2), 351-362.

SOJOUDI, A., SAHA, S.C., XU, F. & GU, Y.T. (2016) Transient air flow and heat transfer due to differential heating on inclined walls and heat source placed on the bottom wall in a partitioned attic shaped space. Energy Building, 113, 39-50.

VAROL, Y., KOCA, A. & OZTOP, H.F. (2006) Natural convection in a triangle enclosure with flush mounted heater on the wall. International Communications in Heat and Mass Transfer, 33 (8), 951-958.

YESILOZ, G. & AYDIN, O. (2013) Laminar natural convection in right-angled triangular enclosures heated and cooled on adjacent walls. International Journal of Heat and Mass Transfer, 60, 365-374.

NOMENCLATURE

g	gravitational acceleration [m/s^2]
k	thermal conductivity [W/m.K]
L	collector width
$\vec{n}$	unit vector normal to the wall
N_s	local generated entropy
Nu	Nusselt number
Pr	Prandtl number
Ra	Rayleigh number
$\vec{q}'$	heat flux vector
S'$_{gen}$	generated entropy
t	dimensionless time ($t'.\alpha/L^2$)
T	dimensionless temperature [$(T'-T'_c)/(T'_h-T'_c)$]
T'_c	cold temperature [K]
T'_h	hot temperature [K]
$\vec{V}$	dimensionless velocity vector (= $\vec{V}'.L/\alpha$)
x, y, z	dimensionless Cartesian coordinates (x'/L, y'/L, z'/L)

Greek symbols

α	thermal diffusivity [m^2/s]
β	thermal expansion coefficient [1/K]

ρ	density [kg/m^3]
μ	dynamic viscosity [kg./m.s]
ν	kinematic viscosity [m^2/s]
φ	irreversibility coefficient
ϕ'	dissipation function
$\vec{\psi}$	dimensionless vector potential ($\vec{\psi}'/\alpha$)
$\vec{\omega}$	dimensionless vorticity ($\vec{\omega}'.\alpha/L^2$)
ΔT	dimensionless temperature difference

Subscripts

x, y, z	Cartesian coordinates
Th	thermal
Fr	friction
Tot	Total
h	Hot
c	Cold
av	average

Superscript

'	dimensional variable